Structural Engineering and Mechanics, Vol. 44, No. 5 (2012) 663-680
DOI: http://dx.doi.org/10.12989/sem.2012.44.5.663

Influence of ground motion spatial variations and local soil conditions on the seismic responses of buried segmented pipelines

Kaiming Bi* and Hong Hao[a]

School of Civil and Resource Engineering, The University of Western Australia, 35 Stirling Highway, Crawley, WA 6009, Australia

(Received August 22, 2012, Revised October 30, 2012, Accepted November 1, 2012)

Abstract. Previous major earthquakes revealed that most damage of the buried segmented pipelines occurs at the joints of the pipelines. It has been proven that the differential motions between the pipe segments are one of the primary reasons that results in the damage (Zerva *et al*. 1986, O'Roueke and Liu 1999). This paper studies the combined influences of ground motion spatial variations and local soil conditions on the seismic responses of buried segmented pipelines. The heterogeneous soil deposits surrounding the pipelines are assumed resting on an elastic half-space (base rock). The spatially varying base rock motions are modelled by the filtered Tajimi-Kanai power spectral density function and an empirical coherency loss function. Local site amplification effect is derived based on the one-dimensional wave propagation theory by assuming the base rock motions consist of out-of-plane SH wave or combined in-plane P and SV waves propagating into the site with an assumed incident angle. The differential axial and lateral displacements between the pipeline segments are stochastically formulated in the frequency domain. The influences of ground motion spatial variations, local soil conditions, wave incident angle and stiffness of the joint are investigated in detail. Numerical results show that ground motion spatial variations and local soil conditions can significantly influence the differential displacements between the pipeline segments.

Keywords: buried segmented pipelines; seismic response; ground motion spatial variation; local site effect; stochastic method

1. Introduction

Buried pipelines were heavily damaged during previous major earthquakes, for example in the 1995 Kobe earthquake (Kuraoka and Rainer 1996), the 1999 Chi-Chi earthquake (Tasi *et al*. 2000) and more recently the 2008 Wenchuan earthquake (Yuan and Sun 2008) and the 2010 Chile earthquake (Tang *et al*. 2010). Based on the damage mechanism of buried pipelines, seismic impacts can be classified into being caused by permanent movements of ground (i.e., surface faulting, landsliding and soil liquefaction induced lateral spreading) or by transient seismic wave

*Corresponding author, Lecturer, E-mail: kaiming.bi@ uwa.edu.au
[a]Winthrop Professor, E-mail: hong.hao@ uwa.edu.au

propagation (i.e., transient strain and curvature in the ground due to travelling wave effects) (O'Rourke and Liu 1999). This paper studies the seismic responses of buried segmented pipelines due to seismic wave propagation effect.

Pipelines are important lifeline structures. They usually extend for long distances along the ground surface. The seismic waves along the pipelines are inevitably different, which is known as the ground motion spatial variations. Many reasons that may cause the ground motion spatial variations such as the wave passage effect resulting from the different arrival times of waves at different locations, coherency loss effect owing to seismic waves scattering in the heterogeneous medium of the ground and site amplification effect due to different local soil properties (Der Kiureghian 1996). Many spatially varying ground motion models have been proposed especially after the installation of the SMART-1 dense array in Lotung, Taiwan. Zerva and Zervas (2002) overviewed these models. Two parts are usually included in these models, the lagged coherency, which measures the similarity of the analysed seismic motions, and the phase spectrum, which depicts the wave passage effect.

Reconnaissance reports revealed that the joints are the most vulnerable parts of the segmented pipelines since large relative displacements usually occur between these segments, and these larger relative displacements in turn lead to the pull-out and shear crack damage at the joints. One of the main reasons that results in the large relative displacement is the ground motion spatial variations. The influence of spatially varying ground motions on the seismic responses of buried segmented pipelines have been studied by some researchers. Nelson and Weidlinger (1979) introduced the interference response spectra in an attempt to take the spatial variation of ground motions into account. The model is based on the differential motion of a two-degree of freedom pipeline, in which two pipe segments behave as rigid bodies that are supported by springs and dashpots. The base motion at the left support is a given acceleration time history, whereas the input at the right support is the same acceleration time history but delayed by the travel time of the motion between the supports. In other words, only the ground motion wave passage effect was considered in the study. Zerva *et al*. (1986) developed a model for the near source ground motions, in which, the excitation is modelled as a random process, the auto and cross power spectral density functions of accelerations at stations on the ground surface are estimated based on the data recorded at the SMART-1 array. The developed model was then applied to stochastically investigate the differential displacements between different segments of buried pipelines (Zerva *et al*. 1986, 1988). However, it should be noted that the SMART-1 array is located at a relatively flat-lying alluvial site, therefore the influence of local soil conditions cannot be considered by using ground motion spatial variation models derived from the recorded spatial ground motions at the SMART-1 array.

Local soil site can filter the frequency contents and amplify the amplitudes of the incoming seismic waves, which in turn further intensifies the ground motion spatial variations. In fact, previous studies reveal that local site effect not only causes further phase difference (Der Kiureghian 1996) but also affects the amplitude of lagged coherency (Bi and Hao 2011). These differences can significantly influence the structural responses (e.g., Zembaty and Rutenburg 2002, Dumanogluid and Soyluk 2003, Bi *et al*. 2010a). As for the buried segmented pipelines, Hadid and Afra (2000) adopted the model proposed by Nelson and Weidlinger (1979) and Zerva *et al*. (1986, 1988), and carried out a sensitivity analysis of site effects on response spectra of pipelines. However, only site amplification effect was considered in their study, the wave passage effect and coherency loss effect were neglected. Moreover, in their numerical model, the stiffness and damping of the soil springs at different supports of the segmented pipelines were assumed to be the same though the soil conditions surrounding the pipelines varied. This is obviously an unrealistic

assumption since the stiffness and damping of the soil spring is undoubtedly related to the soil parameters (Hindy and Novak 1979, Zerva *et al*. 1988). This assumption may lead to inaccurate predictions of pipeline responses.

Based on the discussion above, previous studies on the seismic responses of buried segmented pipelines either neglected ground motion spatial variations (Hadid and Afra 2000) or local site effect (Nelson and Weidlinger 1979, Zerva *et al*. 1986, 1988). A comprehensive consideration of the combined ground motion spatial variations and local soil conditions on the seismic responses of buried segmented pipelines has not been reported. This paper directly relates the coefficients of the springs and dashpots with the surrounding soil properties and studies the combined ground motion spatial variations and local site effects on the seismic responses of buried segmented pipelines. The heterogeneous soil deposits surrounding the pipelines are assumed resting on an elastic half-space (base rock). The spatially varying base rock motions are modelled by the filtered Tajimi-Kanai power spectral density function and an empirical coherency loss function. Local site amplification effect is derived based on the one-dimensional wave propagation theory by assuming the base rock motions consist of out-of-plane SH wave or combined in-plane P and SV waves propagating into the site with an assumed incident angle. The differential axial and lateral displacements between the pipe segments are stochastically formulated in the frequency domain. The influences of various factors that significantly affect the differential displacements at the joint, i.e., ground motion spatial variations, local soil conditions, wave incident angle and stiffness of the joint, are investigated.

2. Structural response equation formulation

The discrete model adopted by Nelson and Weidlinger (1979), Zerva *et al*. (1986, 1988) and Hadid and Afra (2000) is revised in the present study to investigate the differential displacements between the two segments in the axial direction and in the directions normal to the pipeline axis (lateral and vertical directions). In general, the ground motions in the three orthogonal directions are assumed uncorrelated with each other, the structural responses in these three directions thus can be examined independently as suggested by Zerva *et al*. (1986, 1988). Moreover, for the structural responses in the directions normal to the pipeline axis, the same formulations can be applied, and the pipeline response in the vertical direction is usually smaller than that in the lateral direction (Zerva *et al*. 1986, 1988), therefore the structural responses in the vertical direction are not discussed in the present study. The structural responses in the axial and lateral directions are formulated independently in this section.

2.1 Response in the axial direction

Fig. 1 shows the discrete model for differential axial motion across the joint. The two pipeline segments are assumed to behave as rigid bodies, and interconnected by a spring with stiffness k_{pA} and a dashpot with damping c_{pA}. Pipe-soil interactions are represented by springs and dashpots, with k_{g1A} and c_{g1A} for the left segment and k_{g2A} and c_{g2A} for the right segment, respectively. The lengths and masses of the pipeline segments are l and m respectively, the separation distance between the two centroids of the segments is thus also l. The axial displacements of the two pipes are $x_1(t)$ and $x_2(t)$, where $x_{g1}(t)$ and $x_{g2}(t)$ are the axial ground excitations at the two supports. This model is revised from a previous study (Hadid and Afra 2000), in which the coefficients of the soil-pipe

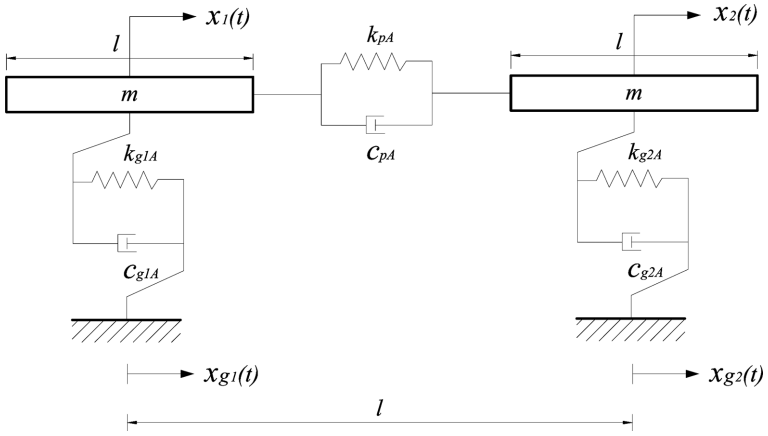

Fig. 1 Discrete model for differential axial motion across the joint (not to scale)

interactions are assumed to be the same for the two supports (i.e., $k_{g1A} = k_{g2A}$ and $c_{g1A} = c_{g2A}$) though different soils surrounding the pipelines are assumed. In the present study, the coefficients of the soil springs directly relate to the surrounding soil properties, with $k_{g1A} = 2G_{s1}$ and $k_{g2A} = 2G_{s2}$ (Zerva *et al*. 1988), where G_{s1} and G_{s2} are the shear moduli of the surrounding soils.

With the numerical model shown in Fig. 1, the equilibrium equation of the system can be written as

$$[M]_A\{\ddot{x}\} + [C]_A\{\dot{x}\} + [K]_A\{x\} = [K_{sb}]_A\{x_g\} + [C_{sb}]_A\{\dot{x}_g\} \tag{1}$$

where

$$[M]_A = \begin{bmatrix} m & 0 \\ 0 & m \end{bmatrix} \tag{2.1}$$

$$[C]_A = \begin{bmatrix} c_{pA} + c_{g1A} & -c_{pA} \\ -c_{pA} & c_{pA} + c_{g2A} \end{bmatrix} \tag{2.2}$$

$$[K]_A = \begin{bmatrix} k_{pA} + k_{g1A} & -k_{pA} \\ -k_{pA} & k_{pA} + k_{g2A} \end{bmatrix} \tag{2.3}$$

$$[K_{sb}]_A = \begin{bmatrix} k_{g1A} & 0 \\ 0 & k_{g2A} \end{bmatrix} \tag{2.4}$$

$$[C_{sb}]_A = \begin{bmatrix} c_{g1A} & 0 \\ 0 & c_{g2A} \end{bmatrix} \tag{2.5}$$

$$\{x\} = [x_1 \;\; x_2]^T \tag{2.6}$$

and

$$\{x_g\} = [x_{g1} \;\; x_{g2}]^T \tag{2.7}$$

with the superscript 'T' denotes a matrix transpose.

Eq. (1) can be decoupled into its modal vibration equation as

$$\ddot{q}_{kA} + 2\xi_{kA}\omega_{kA}\dot{q}_{kA} + \omega_{kA}^2 q_{kA} = \frac{[\varphi_k^T]_A[K_{sb}]_A}{[\varphi_k^T]_A[M]_A[\varphi_k]_A}\{x_g\} + \frac{[\varphi_k^T]_A[C_{sb}]_A}{[\varphi_k^T]_A[M]_A[\varphi_k]_A}\{\dot{x}_g\} \qquad k = 1, 2 \tag{3}$$

where $[\varphi_k]_A$ is the kth vibration mode shape of the system, q_k is the kth modal response, ω_{kA} and ξ_{kA} are the corresponding circular frequency and viscous damping ratio, respectively.

With the stiffness proportional damping, the kth modal response in the frequency domain can be obtained from Eq. (3) as

$$\bar{q}_{kA}(i\omega) = H_{kA}(i\omega)\left[\frac{[\varphi_k^T]_A[K_{sb}]_A}{[\varphi_k^T]_A[M]_A[\varphi_k]_A}\{\bar{x}_g(i\omega)\} + \frac{[\varphi_k^T]_A[C_{sb}]_A}{[\varphi_k^T]_A[M]_A[\varphi_k]_A}\{\dot{\bar{x}}_g(i\omega)\}\right] =$$

$$H_{kA}(i\omega)\left[\frac{1 + 2i\omega\xi_{kA}/\omega_{kA}}{[\varphi_k^T]_A[M]_A[\varphi_k]_A}\right]\{\bar{x}_g(i\omega)\} = H_{kA}(i\omega)\sum_{j=1}^{r}\psi_{kjA}\bar{x}_{gj}(i\omega) \tag{4}$$

in which r is the total number of supports, and

$$H_{kA} = \frac{1}{-\omega^2 + \omega_{kA}^2 + 2i\xi_{kA}\omega_{kA}} \tag{5}$$

is the kth modal frequency response function

$$\psi_{kjA} = \frac{[1 + 2i\omega\xi_{kA}/\omega_{kA}][\varphi_k^T]_A[K_{sb}^j]_A}{[\varphi_k^T]_A[M]_A[\varphi_k]_A} \tag{6}$$

is the participation coefficient for the kth mode corresponding to a movement at support j, $[K_{sb}^j]_A$ is a vector in the stiffness matrix $[K_{sb}]_A$ corresponding to support j.

The structural response of the ith degree of freedom is

$$x_i(t) = \sum_{k=1}^{n}\varphi_{kA}^i q_{kA}(t) \tag{7}$$

where n is the number of modes considered in the calculation, and φ_{kA}^i is the kth mode shape value corresponding to the ith degree of freedom.

For the system shown in Fig. 1, the differential axial displacement between the two pipeline segments is

$$\Delta x = x_1 - x_2 = \sum_{k=1}^{n}(\varphi_{kA}^1 - \varphi_{kA}^2)q_{kA} \tag{8}$$

The power spectral density function of Δx then can be derived as

$$S_{\Delta x} = \frac{1}{\omega^4}[|P_1|^2 S_{x_{g1}} + |P_2|^2 S_{x_{g2}} + 2Re(P_1 P_2^* S_{x_{g1g2}})] \tag{9}$$

where

$$P_1(i\omega) = \sum_{k=1}^{n}(\varphi_{kA}^1 - \varphi_{kA}^2)H_{kA}(i\omega)\psi_{k1A} \tag{10.1}$$

$$P_2(i\omega) = \sum_{k=1}^{n}(\varphi_{kA}^1 - \varphi_{kA}^2)H_{kA}(i\omega)\psi_{k2A} \tag{10.2}$$

$S_{x_{g1}}$ and $S_{x_{g2}}$ are the auto spectral density functions of the axial ground motions at the two supports, $S_{x_{g1g2}}$ is the axial ground motion cross power spectral density function between the two supports. The formulation of them will be discussed in Section 3. 'Re' denotes the real part of a complex quantity and '*' represents complex conjugate. The mean peak response of the differential displacement can be obtained by using the standard random vibration method as will be discussed in Section 4 once the corresponding power spectral density function is formulated.

2.2 Response in the lateral direction

The discrete model used to evaluate the differential lateral displacement between the pipeline segments is shown in Fig. 2. The model is similar to that in Fig. 1. The only difference is that two rotational motions $\theta_1(t)$ and $\theta_2(t)$, one for each pipe segments are also introduced in the model (Zerva *et al*. 1986, 1988). The relation between the soil stiffness and the shear modulus of the surrounding soil is $k_{g1L} = 3G_{s1}$ and $k_{g2L} = 3G_{s2}$ (Zerva *et al*. 1988).

With the numerical model, the equilibrium equation of the system can be written as

$$[M]_L\{\ddot{y}\} + [C]_L\{\dot{y}\} + [K]_L\{y\} = [k_{sb}]_L\{y_g\} + [C_{sb}]_L\{\dot{y}_g\} \tag{11}$$

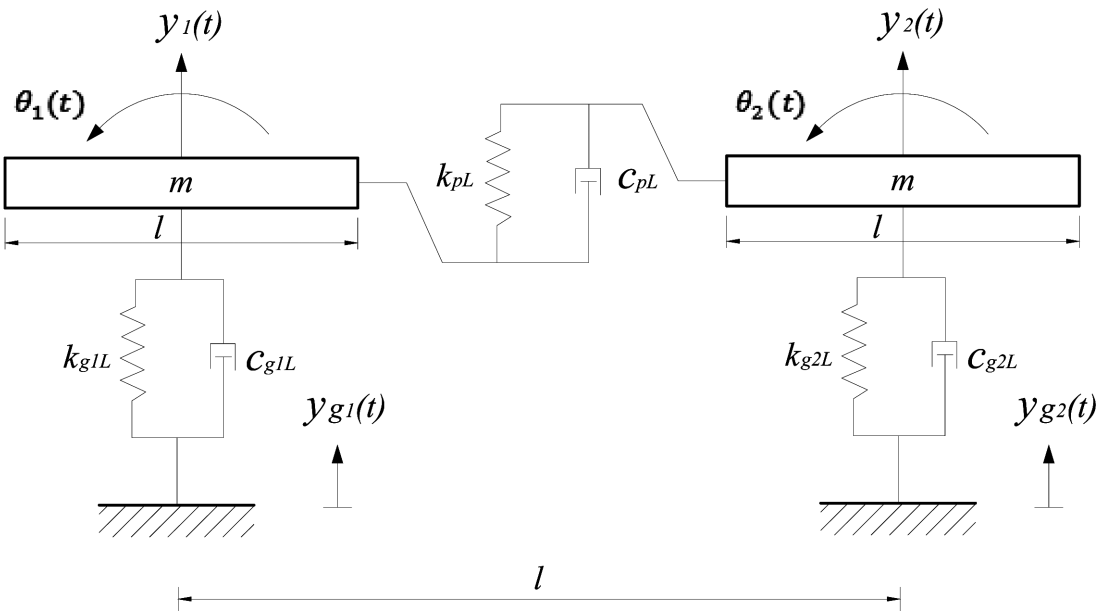

Fig. 2 Discrete model for differential lateral motion across joint (not to scale)

where

$$[M]_L = \begin{bmatrix} m & 0 & 0 & 0 \\ 0 & m & 0 & 0 \\ 0 & 0 & \dfrac{mL^2}{12} & 0 \\ 0 & 0 & 0 & \dfrac{mL^2}{12} \end{bmatrix} \tag{12.1}$$

$$[C]_L = \begin{bmatrix} c_{pL}+c_{g1L} & -c_{pL} & c_{pL}l' & c_{pL}l' \\ -c_{pL} & c_{pL}+c_{g2L} & -c_{pL}l' & -c_{pL}l' \\ c_{pL}l' & -c_{pL}l' & c_{pL}l'^2 & c_{pL}l'^2 \\ c_{pL}l' & -c_{pL}l' & c_{pL}l'^2 & c_{pL}l'^2 \end{bmatrix} \tag{12.2}$$

$$[K]_L = \begin{bmatrix} k_{pL}+k_{g1L} & -k_{pL} & k_{pL}l' & k_{pL}l' \\ -k_{Lp} & k_{pL}+k_{g2L} & -k_{pL}l' & -k_{pL}l' \\ k_{pL}l' & -k_{pL}l' & k_{pL}l'^2 & k_{pL}l'^2 \\ k_{pL}l' & -k_{pL}l' & k_{pL}l'^2 & k_{pL}l'^2 \end{bmatrix} \tag{12.3}$$

$$[K_{sb}]_L = \begin{bmatrix} k_{g1L} & 0 \\ 0 & k_{g2L} \\ 0 & 0 \\ 0 & 0 \end{bmatrix} \tag{12.4}$$

$$[C_{sb}]_L = \begin{bmatrix} c_{g1L} & 0 \\ 0 & c_{g2L} \\ 0 & 0 \\ 0 & 0 \end{bmatrix} \tag{12.5}$$

$$\{y\} = [y_1 \;\; y_2 \;\; \theta_1 \;\; \theta_2]^T \tag{12.6}$$

and

$$\{y_g\} = [y_{g1} \;\; y_{g2}]^T \tag{12.7}$$

with $l' = l/2$.

Similar to Eq. (4), the kth modal response in the frequency domain can be obtained as

$$\bar{q}_{kL}(i\omega) = H_{kL}(i\omega)\sum_{j=1}^{r}\psi_{kjL}\bar{y}_{gj}(i\omega) \quad k = 1, \ldots, 4 \tag{13}$$

with

$$H_{kL} = \frac{1}{-\omega^2 + \omega_{kL}^2 + 2i\xi_{kL}\omega_{kL}} \tag{14}$$

representing the kth modal frequency response function, and

$$\psi_{kjL} = \frac{[1 + 2i\omega\xi_{kL}/\omega_{kL}][\varphi_k^T]_L[K_{sb}^j]_L}{[\varphi_k^T]_L[M]_L[\varphi_k]_L} \tag{15}$$

denoting the participation coefficient.

The differential lateral displacement between the two pipeline segments is

$$\Delta y = y_1 - y_2 + l'(\theta_1 + \theta_2) = \sum_{k=1}^{n}[\varphi_{kL}^1 - \varphi_{kL}^2 + l'(\varphi_{kL}^3 + \varphi_{kL}^4)]q_{kL} \tag{16}$$

The power spectral density function of Δy then can be derived as

$$S_{\Delta y} = \frac{1}{\omega^4}[|P_3|^2 S_{y_{g1}} + |P_4|^2 S_{y_{g2}} + 2Re(P_3 P_4^* S_{y_{g1g2}})] \tag{17}$$

where

$$P_3(i\omega) = \sum_{k=1}^{n}[\varphi_{kL}^1 - \varphi_{kL}^2 + l'\varphi_{kL}^3 + l'\varphi_{kL}^4]H_{kL}(i\omega)\psi_{k1L} \tag{18.1}$$

$$P_4(i\omega) = \sum_{k=1}^{n}[\varphi_{kL}^1 - \varphi_{kL}^2 + l'\varphi_{kL}^3 + l'\varphi_{kL}^4]H_{kL}(i\omega)\psi_{k2L} \tag{18.2}$$

with $S_{y_{g1}}$, $S_{y_{g2}}$ and $S_{y_{g1g2}}$ denoting the auto and cross power spectral density functions of the lateral ground surface motions.

3. Spatial ground motion model

According to Eq. (9) and Eq. (17), the power spectral density functions of differential displacements in the axial and lateral directions can be formulated when the corresponding auto and cross power spectral density functions of the ground motions are known. For a single soil layer resting on an elastic half space, the spatially varying surface motions can be formulated based on the combined one-dimensional wave propagation theory and spectral representation method (Bi and Hao 2012), which is briefly introduced in this section.

3.1 Base rock motion

Fig. 3 shows a single soil layer resting on an elastic half space (base rock). The shear modulus, density, depth, damping ratio and Poisson's ratio for the soil layer are G_s, ρ_s, h_s, ξ_s and υ_s, respectively. The corresponding values on the base rock are G_R, ρ_R, ξ_R and υ_R. The base rock motions are assumed consisting of out-of-plane SH wave and combined in-plane P and SV waves propagating into the site with an assumed incident angle α.

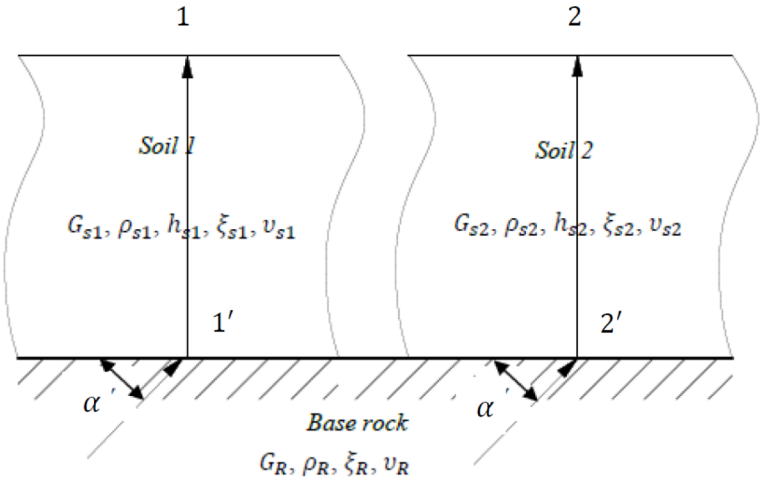

Fig. 3 A single soil layer resting on an elastic half space

The motion on the base rock (Points 1' and 2' in Fig. 3) is assumed to have the same intensity and frequency contents, and is modelled by a filtered Tajimi-Kanai power spectral density function as

$$S_g(\omega) = \frac{\omega^4}{(\omega_f^2-\omega^2)^2+(2\omega_f\omega\xi_f)^2}\,\frac{1+4\xi_g^2\omega_g^2\omega^2}{(\omega_g^2-\omega^2)^2+4\xi_g^2\omega_g^2\omega^2}\Gamma \tag{19}$$

where ω_g and ξ_g are the central frequency and damping ratio of the Tajimi-Kanai power spectral density function, ω_f and ξ_f are the corresponding central frequency and damping ratio of the high pass filter function. Γ is a scaling factor depending on the ground motion intensity. The parameters for the base rock motions are assumed as $\omega_g = 10\pi$ rad/s, ξ_g = 0.6, $\omega_f = 0.5\pi$, ξ_f = 0.6 and $\Gamma = 0.022$ m^2/s^3. These parameters correspond to a ground motion time history with duration $T = 20$ s and PGA of 0.5 g based on the standard random vibration method (Der Kiureghian 1980) as will be discussed in Section 4.

The incoherency and wave passage effects of the motions on the base rock are represented by an empirical coherency loss function, and the Sobczyk model (Sobczyk 1991) is selected

$$\gamma_{1'2'}(i\omega) = |\gamma_{1'2'}(i\omega)|\exp(-i\omega d_{1'2'}\cos\alpha/v_{app}) = \exp(-\beta\omega d_{1'2'}^2/v_{app})\cdot\exp(-i\omega d_{1'2'}\cos\alpha/v_{app}) \tag{20}$$

where α is the incident angle, β is a coefficient which reflects the level of coherency loss, $d_{1'2'} = l$ is the distance between the centroid of the two pipe segments. v_{app} is the apparent wave velocity at the base rock, which is related to the base rock properties and the specified incident angle.

3.2 Local site effect

The one-dimensional (1D) wave propagation theory proposed by Wolf (1985) is adopted in the present study to consider the influence of local soil conditions. In this theory, the seismic waves

propagate with an incident angle α on the base rock and then propagate vertically into the soil layer as shown in Fig. 3.

For a harmonic excitation with frequency ω, the dynamic equilibrium equations can be written as (Wolf 1985)

$$\nabla^2 e = -\frac{\omega^2}{c_p^2} e \quad \text{or} \quad \nabla^2 \{\Omega\} = -\frac{\omega^2}{c_s^2} \{\Omega\} \tag{21}$$

where $\nabla^2 e$ and $\nabla^2 \{\Omega\}$ are the Laplace operator of the volumetric strain amplitude e and rotational-strain-vector $\{\Omega\}$. c_p and c_s are the P- and S-wave velocity, respectively. This equation can be solved by using the P- and S-wave trial function. The out-of-plane displacements is caused by the incident SH wave, while the in-plane horizontal displacement depends on the combined P and SV waves. The out-of-plane motion is independent of in-plane motion, hence, the two-dimensional dynamic stiffness matrix of the soil layer for the out-of-plane and in-plane motion, $[S_{SH}^L]$ and $[S_{P-SV}^L]$, can be formulated independently by analysing the relations of shear stresses and displacements at the boundary of the soil layer. Assembling the matrices of the soil layer and the base rock, the dynamic stiffness of the total system is obtained and denoted by $[S_{SH}]$ and $[S_{P-SV}]$, respectively. The dynamic equilibrium equation of the site in the frequency domain is thus (Wolf 1985)

$$[S_{SH}]\{u_{SH}\} = \{P_{SH}\} \quad \text{or} \quad [S_{P-SV}]\{u_{P-SV}\} = \{P_{P-SV}\} \tag{22}$$

where $\{u_{SH}\}$ and $\{P_{SH}\}$ are the out-of-plane displacements and load vector corresponding to the incident SH wave, $\{u_{P-SV}\}$ and $\{P_{P-SV}\}$ are the in-plane displacements and load vector of the combined P and SV waves. The stiffness matrices $[S_{SH}]$ and $[S_{P-SV}]$ depend on soil properties, incident wave type, incident angle and circular frequency ω. The dynamic load $\{P_{SH}\}$ and $\{P_{P-SV}\}$ depend on the base rock properties, incident wave type, incident wave frequency and amplitude. By solving Eq. (22) in the frequency domain at every discrete frequency, the relationship of the amplitudes between the base rock and each soil layer can be formed, and the site transfer functions in the in-plane (H_{sA}) and out-of-plane (H_{sL}) directions can be estimated.

3.3 Spatially varying ground surface motions

After obtaining the ground motions on the base rock and the transfer functions of local soil sites, the spatially varying axial motions on the ground surface then can be formulated as (Bi and Hao 2012)

$$\begin{aligned} S_{x_{g1}} &= \left|H_{sA1}(i\omega)\right|^2 S_g(\omega) \\ S_{x_{g2}} &= \left|H_{sA2}(i\omega)\right|^2 S_g(\omega) \\ S_{x_{g1g2}} &= H_{sA1}(i\omega) H_{sA2}^*(i\omega) S_g(\omega) \gamma_{1'2'}(i\omega) \end{aligned} \tag{23}$$

And similarly, the spatially varying lateral motions on the ground surface are

$$S_{y_{g1}} = |H_{sL1}(i\omega)|^2 S_g(\omega)$$

$$S_{y_{g2}} = |H_{sL2}(i\omega)|^2 S_g(\omega)$$

$$S_{y_{g1g2}} = H_{sL1}(i\omega) H^*_{sL2}(i\omega) S_g(\omega) \gamma_{1'2'}(i\omega) \tag{24}$$

4. Maximum response calculation

The mean peak differential axial and lateral displacements between the pipe segments can be estimated by the standard random vibration method (Der Kiureghian 1980).

For a zero mean stationary process $\mu(t)$ with known power spectral density function $S(\omega)$, its mth order spectral moment is defined as

$$\lambda_m \approx \int_0^{\omega_c} \omega^m S(\omega) d\omega \tag{25}$$

where ω_c is a high cut-off frequency.

The zero mean cross rate v and shape factor of the power spectral density function δ, can be obtained by

$$v = \frac{1}{\pi}\sqrt{\frac{\lambda_2}{\lambda_0}} \tag{26}$$

$$\delta = \sqrt{1 - \frac{\lambda_1^2}{\lambda_0 \lambda_2}} \tag{27}$$

the mean peak response can then be calculated by

$$\mu_{\max} = \left(\sqrt{2\ln v_e T} + \frac{0.5772}{\sqrt{2\ln v_e T}}\right)\sigma \tag{28}$$

where T is the duration of the stationary process, $\sigma = \sqrt{\lambda_0}$ is the standard deviation of the process, and

$$v_e T = \begin{cases} \max(2.1, 2\delta T) & 0 \le \delta < 0.1 \\ (1.63\delta^{0.45} - 0.38) vT & 0.1 \le \delta < 0.69 \\ vT & \delta \ge 0.69 \end{cases} \tag{29}$$

In the present study, the high cut-off frequency is taken as 50 Hz since it covers the predominant vibration modes of most engineering structures and the dominant earthquake ground motion frequencies.

5. Numerical results

Two segmented steel pipelines connected by a joint are selected as an example. The mass density of the pipe = 7800 kg/m^3, length l = 100 m, inner diameter = 0.6 m and outer diameter = 0.61 m. The segmented pipelines are buried in a heterogeneous soil layer resting on an elastic half space as shown in Fig. 3. The properties of soil 1 are G_{s1} = 40 MPa, ρ_{s1} = 1600 kg/m^3, h_{s1} = 50 m, ξ_{s1} = 5% and υ_{s1} = 0.4, and those for the base rock are G_R = 1800 MPa, ρ_R = 2500 kg/m^3, ξ_R = 5% and υ_R = 0.33, respectively. To study the influence of different soil conditions, the properties of soil 2 vary in the present study. In particular, the shear modulus of soil 2 varies from 20 to 160 MPa, while other parameters are the same as soil 1. Another factor, which significantly influences the structural response, is the stiffness of the joint. For simplicity, following two parameters are defined

$$\chi = \frac{k_{g2A}}{k_{g1A}} = \frac{k_{g2L}}{k_{g1L}}, \quad \eta = \frac{k_{pA}}{k_{g1A}} = \frac{k_{pL}}{k_{g1L}} \tag{30}$$

These two parameters describe the relation between the stiffness of the supporting soils and that between the joint and the soil. The influences of ground motion spatial variations, local soil conditions, wave incident angle and joint stiffness are investigated in detail in this section.

5.1 Influence of ground motion spatial variations

To investigate the influence of ground motion spatial variations, highly (β = 0 in Eq. (20), which is also known as wave passage effect), intermediately (β = 0.001) and weakly (β = 0.002) correlated ground motions are investigated. For comparison purpose, uniform excitations (β = 0 and $v_{app} = \infty$) are also considered. To preclude the influences of other parameters, the incident angle is assumed to be α = 45° and the stiffness ratio between the joint and soil 1 is η = 0.2. Fig. 4 shows the different coherency loss functions.

The effect of ground motion spatial variations on the differential axial and lateral displacements across the joint is shown in Fig. 5 and Fig. 6 respectively. The corresponding standard deviations,

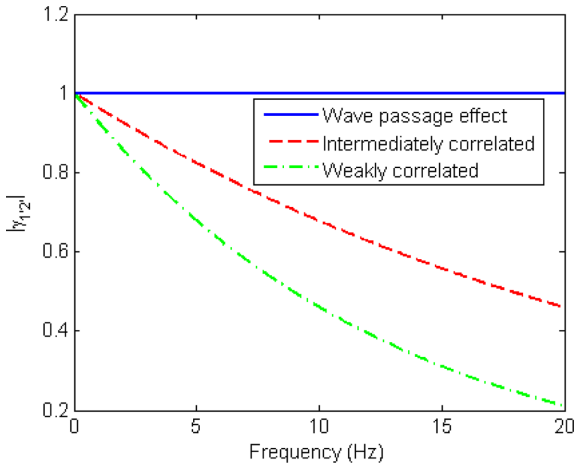

Fig. 4 Different coherency loss functions

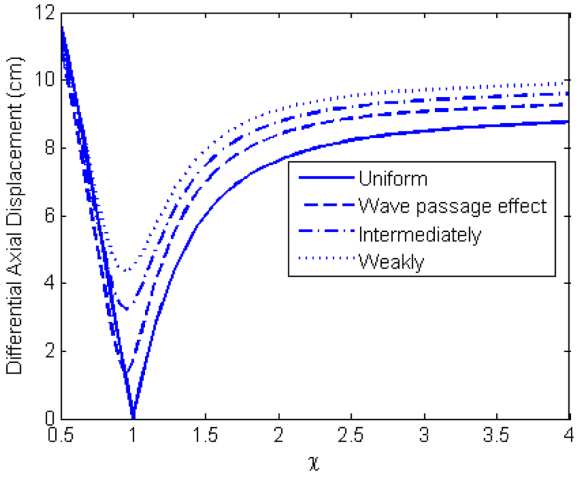

Fig. 5 Influence of ground motion spatial variations on the differential axial displacement across the joint

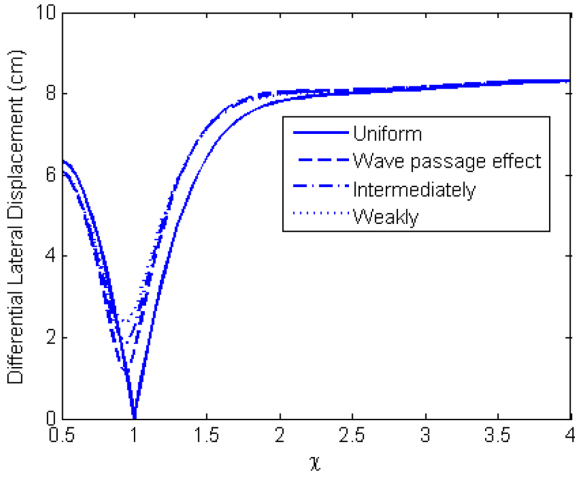

Fig. 6 Influence of ground motion spatial variations on the differential lateral displacement across the joint

which are not shown here, are rather small as compared to the mean peak responses. Therefore, only the mean peak responses are presented and discussed hereafter.

As shown in Fig. 5, with an assumption of uniform excitation, the differential axial displacement between the pipeline segments is relatively small when the soil conditions surrounding the two pipelines are similar, and is zero when $\chi = 1$. This is because the vibration modes of the two segments are exactly the same and the two segments will vibrate in phase in this case. Therefore, there is no relative displacement between them. Spatially varying ground motions can significantly influence the differential axial displacement between the segments, especially when the soil conditions at the two sites are similar. Contrast to the uniform excitation, the minimum relative displacement does not exactly occur at $\chi = 1$, but slightly smaller than unity at $\chi = 0.9$. This is because the two segments are connected by the spring and dashpot system as shown in Fig. 1. This connecting device results in the two vibration frequencies of the system are not exactly $\sqrt{k_{g1A}/m}$ and $\sqrt{k_{g2A}/m}$, which in turn leads to the minimum relative displacement does not exactly occur when $k_{g1A} = k_{g2A}$ ($\chi = 1$). This observation agrees with that by Bi *et al.* (2010b), where they investigated the connecting effect of bearings on a two-span simply-supported bridge structure. Fig. 5 also shows that the ground motion spatial variation effect is most significant when χ is close to unity, and weakly correlated ground motions cause larger relative displacement than highly correlated ground motions. When soil 2 is much stiffer than soil 1, e.g., when $\chi > 2$, the influence of soil conditions on the differential axial displacement is relatively small since the value is almost a constant as shown in Fig. 5. This is because the total response of the structure can be divided into dynamic response and quasi-static response (Clough and Penzien 1993). When soil 2 is stiff enough, the response of the right segment (surrounded by soil 2) is mainly determined by the quasi-static response and the quasi-static response is independent of the structural frequency and is only related to the ground displacement (e.g., Hao 1993, Bi *et al.* 2010a). Fig. 7 shows the mean peak ground displacement of soil 2 with respect to χ. As shown, the ground displacement is almost a constant when $\chi > 2$, which in turn results in the constant relative axial displacement between the two segments in Fig. 5.

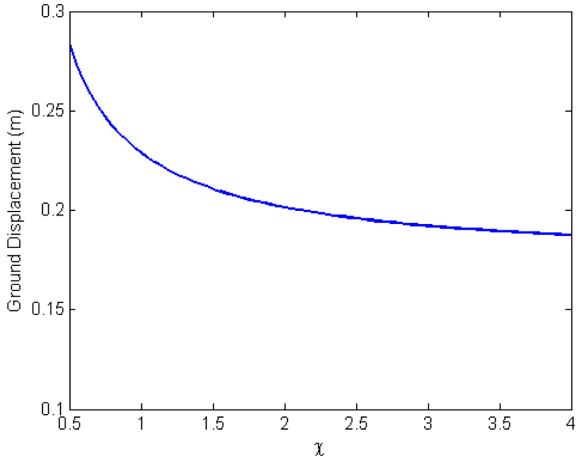

Fig. 7 Mean peak ground displacement of site 2

For the differential lateral displacement as shown in Fig. 6, similar conclusions can be obtained. Namely, ground motion spatial variations can significantly influence the differential lateral displacement especially when χ is close to unity. Contrast to the axial response, the influence of ground motion spatial variations on the lateral displacement can be neglected when the soil conditions surrounding the two pipe segments differ from each other significantly, for example, uniform excitation can give a good prediction of the differential lateral response if $\chi < 0.8$ and $\chi > 2$. This might be because of the contribution of the rotational degrees of freedom.

5.2 Influence of incident angle

The incident angle of the seismic waves on the base rock can significantly influence the differential displacements between the pipeline segments because it affects the wave propagating into the soil layer. To study the influence of incident angle, three different angles are considered, i.e., $\alpha = 20^o$, 45^o and 70^o. The ground motions are assumed to be intermediately correlated ($\beta = 0.001$) and $\eta = 0.2$ is assumed.

Fig. 8 and Fig. 9 show the influence of incident angle on the differential axial and lateral displacements respectively. It is obvious that larger incident angle results in larger differential displacements. This can be explained by the influence of incident angle on the amplification spectra of local soil site as shown in Fig. 10 and Fig. 11. In which, the transfer functions of site 1 in the horizontal in-plane (axial direction) and out-of-plane (lateral direction) directions with different incident angles are plotted respectively. As shown in Fig. 10 and Fig. 11, larger incident angle leads to larger site transfer functions, and thus results in larger ground surface motions (Eq. (23) and Eq. (24)). These larger ground surface motions in turn cause relatively larger differential displacements between the pipeline segments. It should be noted that larger incident angle leads to smaller phase difference between ground motions at two sites as defined in Eq. (20). Smaller spatial ground motion phase difference usually causes less relative structural displacement response. However, the above results indicate that a site amplification of ground motions dominates the relative responses between two pipe segments over the spatial ground motion phase difference associated with larger incident angles.

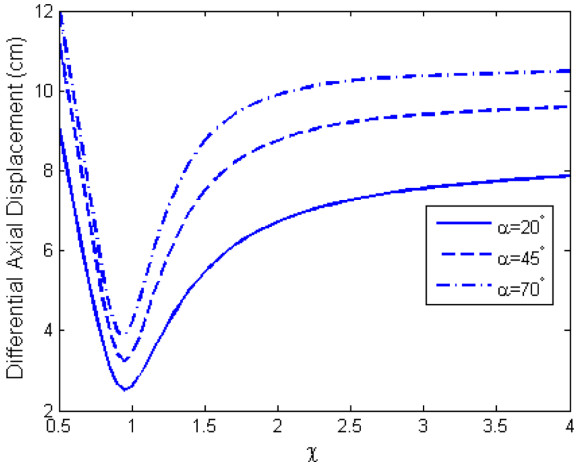

Fig. 8 Influence of incident angle on the on the differential axial displacement across the joint

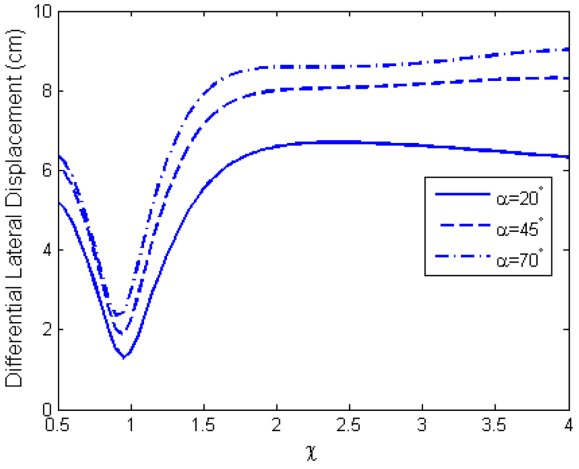

Fig. 9 Influence of incident angle on the differential lateral displacement across the joint

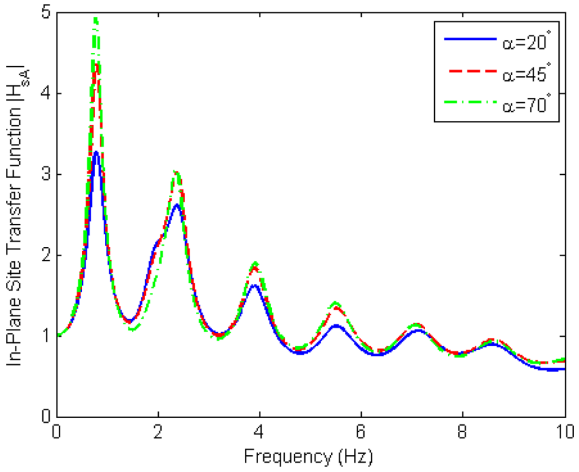

Fig. 10 Influence of incident angle on the horizontal in-plane site transfer function

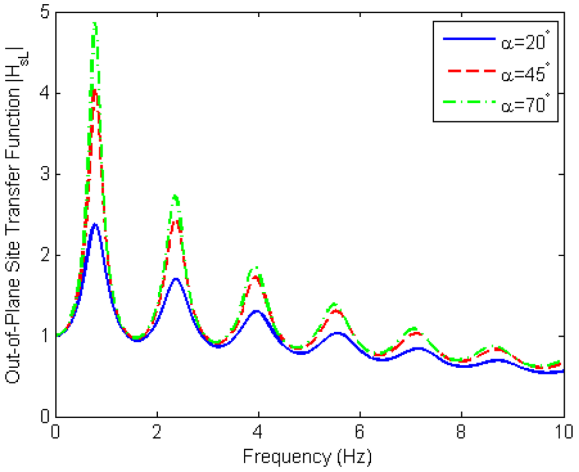

Fig. 11 Influence of incident angle on the horizontal out-of-plane site transfer function

5.3 Influence of joint stiffness

The stiffness of the joint is another factor which significantly influences the differential displacements between the pipe segments. To study the influence of the joint stiffness, three different stiffness ratios, i.e., $\eta = 0.1$, 0.2 and 0.4 are considered, which represent soft, medium and stiff joints respectively. The incident angle of $\alpha = 45^{o}$ and intermediately correlated ground motions ($\beta = 0.001$) are used in the analysis.

Fig. 12 and Fig. 13 show the influence of joint stiffness on the differential axial and lateral displacements between the pipeline segments. As shown, the influence of joint stiffness is prominent. As expected, the softer is the joint, the larger is the differential displacements. When soft

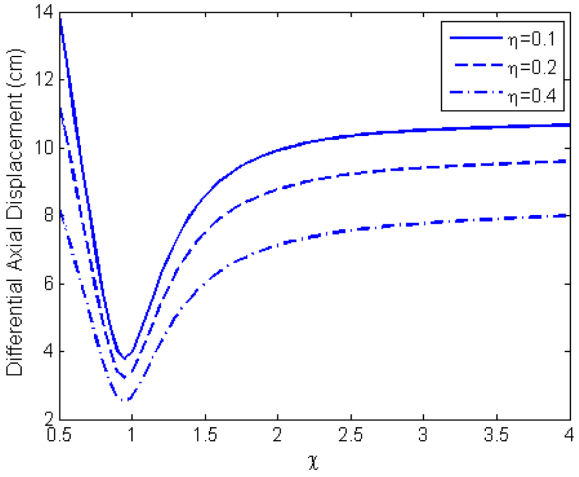

Fig. 12 Influence of joint stiffness on the differential axial displacement across the joint

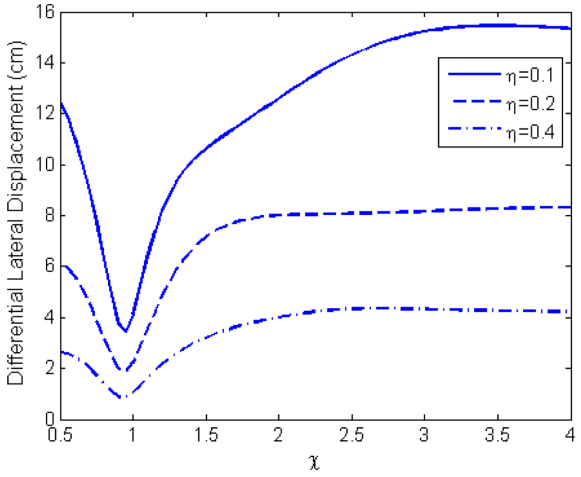

Fig. 13 Influence of joint stiffness on the differential lateral displacement across the joint

joint is considered, the two pipeline segments tend to vibrate freely, large relative displacements thus can be generated. When the joint is stiff enough, the two pipeline segments are likely to vibrate as a whole system, the vibration of the left pipeline is influenced by the right segment, and vice versa. Therefore, smaller relative displacements are anticipated. These observations suggest that increasing the stiffness of the joint is an effective way to mitigate the large relative displacements between the pipeline segments. Considering a particular case, if the joint has the same stiffness as the pipe, the two pipelines can be regarded as a continuous pipeline. In this case, the relative displacements between these two segments will be zero, which indicates that continuous pipeline might be an effective method to avoid the pull-out and shear crack damage of the segmented pipelines.

6. Conclusions

Earthquake induced damage to pipeline was observed in many previous major earthquakes. For buried segmented pipelines, the joint is the most vulnerable part since large relative displacements between the pipeline segments usually result in the pull-out and shear crack damage of the joint. This paper studies the differential axial and lateral displacements between segmented pipelines buried in a heterogeneous soil site resting on an elastic half space. Compared with previous studies, the combined influences of ground motion spatial variations and local soil conditions are considered, and the soil-pipe interaction coefficients are directly related to the supporting soils. This paper is thus believed more realistically modelled the seismic responses of buried segmented pipelines. The influences of ground motion spatial variations, local soil conditions, wave incident angles and joint stiffness are investigated in detail in the paper. Following conclusions can be obtained based on the numerical results:

1. Ground motion spatial variations can significantly influence the differential displacements between the pipeline segments especially when the soil conditions surrounding the two pipelines

are close to each other. Uniform excitation usually underestimates the differential displacements and weakly correlated ground motions generally lead to the largest structural responses.

2. The influence of wave incident angle on the relative displacements at the joints is obvious. Larger incident angle results in larger differential displacements.

3. Joint stiffness prominently influences the differential displacements. Softer joint causes larger relative responses. Stiff joint might be an effective method to avoid the damage at the joints of segmented pipelines.

It should be noted that this paper mainly focuses on the influence of seismic context (ground motion spatial variation and local site effect) on the buried segmented pipelines other than the pipeline itself, the pipe segments were simply modelled as rigid bodies and the connecting joint was represented by a spring-damper system. This simplified model might not be able to explain all types of pipeline, e.g., slip-joint or ductile pipes. Further studies need to be carried out with more realistic pipeline models. Moreover, the responses in the axial direction and lateral direction are assumed independent with each other in the present study. For long pipe segments, the coupling effect might be evident. A more detailed investigation on the coupling effect is also suggested.

Acknowledgements

The authors acknowledge the partial financial support from ARC Linkage Project LP110200906 for carrying out this research.

References

Bi, K. and Hao, H. (2011), "Influence of irregular topography and random soil properties on coherency loss of spatial seismic ground motions", *Earthq. Eng. Struct. D.,* **40**(9), 1045-1061.

Bi, K. and Hao, H. (2012), "Modelling and simulation of spatially varying earthquake ground motions at sites with varying conditions", *Probab. Eng. Mech.,* **29**, 92-104.

Bi, K., Hao, H. and Ren, W. (2010a), "Response of a frame structure on a canyon site to spatially varying ground motions", *Struct. Eng. Mech.,* **36**(1), 111-127.

Bi, K., Hao, H. and Chouw, N. (2010b), "Required separation distance between decks and at abutments of a bridge crossing a canyon site to avoid seismic pounding", *Earthq. Eng. Struct. D.,* **39**(3), 303-323.

Clough, R.W. and Penzien, J. (1993), *Dynamics of Structures*, Second Edition, McGraw-Hill, New York.

Der Kiureghian, A. (1980), "Structural response to stationary excitation", *J. Eng. Mech.,* **106**(6), 1195-1213.

Der Kiureghian, A. (1996), "A coherency model for spatially varying ground motions", *Earthq. Eng. Struct. D.,* **25**(1), 99-111.

Dumanogluid, A.A. and Soyluk, K. (2003), "A stochastic analysis of long span structures subjected to spatially varying ground motions including the site-response effect", *Eng. Struct.,* **25**(10), 1301-1310.

Hadid, M. and Afra, H. (2000), "Sensitivity analysis of site effects on response spectra of pipelines", *Soil Dyn. Earthq. Eng.,* **20**(1-4), 249-260.

Hao, H. (1993), "Arch responses to correlated multiple excitations", *Earthq. Eng. Struct. D.,* **22**(5), 389-404.

Hindy, A. and Novak, M. (1979), "Earthquake response of underground pipelines", *Earthq. Eng. Struct. D.,* **7**(5), 451-476.

Kuraoka, S. and Rainer, J.H. (1996), "Damage to water distribution system caused by the 1995 Hyogo-Ken Nanbu earthquake", *Can. J. Civil Eng.,* **23**(3), 665-677.

Nelson, I. and Weidlinger, P. (1979), "Dynamic seismic analysis of long segmented lifelines", *J. Press. Vess. T.,* **101**, 10-20.

O'Roueke, M.J. and Liu, X. (1999), *Response of Buried Pipelines Subjected to Earthquake Effects*, Multidisciplinary Centre for Earthquake Engineering Research, Monograph Series, No. 3.

Sobczky, K. (1991), *Stochastic Wave Propagation*, Kluwer Academic Publishers, Netherlands.

Tang, A. *et al.* (2010), "Preliminary report on the 27 February 2010 Mw8.8 offshore Maule, Chile earthquake", The Earthquake Engineering Online Archive (NISEE e-library), available online: http://nisee.berkeley.edu/elibrary/Text/201104281.

Tsai, J.S., Jou, L.D. and Lin, S.H. (2000), "Damage to buried water supply pipelines in the Chi-Chi (Taiwan) earthquake and a preliminary evaluation of seismic resistance of pipe joints", *J. Chin. Inst. Eng.,* **23**(4), 395-408.

Wolf, J.P. (1985), *Dynamic Soil-structure Interaction*, Prentice Hall, Englewood Cliffs, New Jersey, USA.

Yuan, Y. and Sun, B. (2008), "General information of engineering damage of Wenchuan Ms 8.0 earthquake", *J. Earthq. Eng. Eng. Vib.,* **28**, 1-114.

Zembaty, Z. and Rutenburg, A. (2002), "Spatial response spectra and site amplification effect", *Eng. Struct.,* **24**(11), 1485-1496.

Zerva, A., Ang, A. H.S. and Wen, Y.K. (1986), "Development of differential response spectra for lifeline seismic analysis", *Probab. Eng. Mech.,* **1**(4), 202-218.

Zerva, A., Ang, A. H.S. and Wen, Y.K. (1988), "Lifeline response to spatially variable ground motions", *Earthq. Eng. Struct. D.,* **16**(3), 361-379.

Zerva, A. and Zervas, V. (2002), "Spatial variation of seismic ground motions: an overview", *Appl. Mech. Rev.*, **55**(3), 271-297.